HHS Public Access

Author manuscript

Nat Genet. Author manuscript; available in PMC 2010 January 01.

Published in final edited form as:

Nat Genet. 2009 July ; 41(7): 793–799. doi:10.1038/ng.400.

Wnt9b signaling regulates planar cell polarity and kidney tubule morphogenesis

Courtney M. Karner[1,2], **Rani Chirumamilla**[1,2], **Shigehisa Aoki**[1,4], **Peter Igarashi**[1,3], **John B. Wallingford**[5], and **Thomas J. Carroll**[1,2,*]

[1]Department of Internal Medicine, Division of Nephrology, University of Texas Southwestern Medical Center, Dallas, TX 75390 USA

[2]Department of Molecular Biology, University of Texas Southwestern Medical Center, Dallas, TX 75390 USA

[3]Department of Pediatrics, University of Texas Southwestern Medical Center, Dallas, TX 75390 USA

[4]Department of Pathology & Biodefense, Faculty of Medicine, Saga University, Saga, Japan

[5]Department of Molecular, Cell and Developmental Biology & Institute for Cellular and Molecular Biology, University of Texas, Austin, Austin, Texas 78712, USA

Abstract

Although many vertebrate organs, such as kidneys, lungs and liver, are composed of epithelial tubules, little is known of the mechanisms that establish the length or diameter of these tubules. In the kidney, defects in the establishment and/or maintenance of tubule diameter are associated with one of the most common inherited human disorders, polycystic kidney disease. Here, we show that attenuation of Wnt9b signaling during kidney morphogenesis affects the planar cell polarity of the epithelium and leads to tubules with significantly increased diameter. Although previous studies showed that polarized cell divisions maintain the diameter of postnatal kidney tubules, we find cell divisions are randomly oriented during embryonic development. Our data suggest that diameter is established during early morphogenetic stages by convergent extension processes and maintained by polarized cell divisions. Wnt9b, signaling through the non-canonical Rho/Jnk branch of the Wnt pathway, is necessary for both of these processes.

*Author for correspondence: Thomas J. Carroll, Departments of Internal Medicine (Nephrology) and Molecular Biology, University of Texas Southwestern Medical Center, Dallas, 5323 Harry Hines Blvd., Dallas, TX 75390-8856, Tel: 214-648-2680, Thomas.carroll@utsouthwestern.edu.

Author Contributions

CMK designed experiments, performed experiments, assembled data and wrote the manuscript, RC performed biochemistry, SA assisted with quantitative analysis on Wnt9b$^{neo/neo}$ kidneys, PI provided KspCre mice and commented on manuscript, JBW assisted with cell orientation analysis, TJC performed initial experiments, designed experiments and wrote manuscript.

Introduction

Epithelial and endothelial tubules are some of the most common structures in the vertebrate body plan. Alterations in the shape of these structures have significant impact on their function. For instance, the functional unit of the kidney, the nephron, is a vascularized epithelial tubule whose proper three-dimensional structure is essential for its function in maintaining body fluid composition1. Defects in the establishment or maintenance of nephron diameter play causal roles in one of the most common genetic maladies in humans, polycystic kidney disease 2. Studies in mice and humans have suggested that increased rates of cell proliferation are associated with, and may directly cause, cyst formation 2,3. However, examination of the developing epithelial tubules of worms and flies indicate that cellular processes that are independent of changes in cell number (e.g. cell size, membrane biosynthesis, cell polarity and cell movements) have significant impact on the establishment and maintenance of tubular diameter 4–15.

The Wnts encode a family of secreted glycolipoproteins that function in multiple biological processes including embryonic development and disease pathogenesis 16. Previous studies have indicated that tight regulation of Wnt signaling is essential for proper development of the kidney tubules. Loss of canonical Wnt signaling in mice prevents formation of the tubules, while inappropriate activation of the Wnt signal transduction pathway leads to cyst formation 17–19. In fact, improper stimulation of the canonical Wnt pathway is a hallmark of various types of human cystic kidney diseases 20. However, recent studies have suggested that defects in planar cell polarity (PCP), a process that may be regulated by non-canonical (b-catenin independent) Wnt signaling may also contribute to cystogenesis 21.

PCP describes the polarization of cells perpendicular to their apical/basal axis 22. Genetic screens in Drosophila have identified multiple factors that are required for the establishment of PCP including two components of the Wnt pathway, Frizzled (Fz) and Dishevelled (Dsh) 23,24. Whether Wnt ligands play a direct role in establishing PCP is somewhat controversial 22,25–28.

We previously showed that Wnt9b was necessary for the earliest events in the induction of the kidney tubules17. Here, we demonstrate that Wnt9b is also required for morphogenesis of the nephron. Wnt9b produced by the ureteric bud and collecting ducts is required autonomously and non-autonomously for proper planar cell polarity within the collecting ducts and the adjacent proximal tubules, respectively. Specifically, we show that these tubules develop in two distinct phases. During the first phase, cell division is not oriented but the diameter of the epithelium decreases. We propose that convergent extension like processes drive the lengthening and thinning of the tubules and establish diameter. In the second phase, polarized cell divisions predominate and maintain tubule diameter. We have found that Wnt9b regulates both phases of development, perhaps through a role in regulating cell orientation. In contrast to its role in tubule induction, Wnt9b's role in tubule morphogenesis is mediated by the non-canonical/planar cell polarity signal transduction branch. This study is the first demonstration that loss of non-canonical Wnt signaling can contribute to cystogenesis as well as the first indication that convergent extension processes regulate tubule diameter in a vertebrate.

Results

Attenuation of Wnt9b signaling leads to dysplastic/cystic kidneys

Embryos completely lacking functional Wnt9b fail to form kidneys, resulting in death on P1. Mice that are homozygous for a hypomorphic (see supplementary note) allele of Wnt9b ($Wnt9b^{neo/neo}$) survive for several days to weeks post partum although 100% (N>30) of $Wnt9b^{neo/neo}$ animals die within 1 month of birth. Gross examination of a P30 mutant kidney revealed that it contained severely dilated/cystic tubules (Figure 1f) indicating that Wnt9b was required for proper establishment and/or maintenance of tubule diameter.

To test if the $Wnt9b^{neo/neo}$ cystic phenotype was the result of a direct role for Wnt9b in tubule diameter regulation rather than a secondary effect caused by deficits in renal vesicle induction, we attempted to specifically ablate Wnt9b from the collecting duct stalks, the cells we hypothesized were the source of Wnt9b during tubule maturation/morphogenesis (to see expression of Wnt9b, view Supplementary figure 1). To accomplish this, we crossed a conditionally inactive (floxed) allele of Wnt9b with mice carrying KspCre29. We found that, similar to what has been described for expression of Ksp-cadherin protein (cadh16) in the rabbit30, the Ksp promoter drives expression of Cre recombinase in the collecting duct stalks but not in the ureteric bud tips at least through E15.5 (Supplementary figure 2a, b, d, e and g and data not shown).

Although Wnt9b null kidneys do not branch or induce a mesenchymal to epithelial transition 17, KspCre;$Wnt9b^{-/flox}$ kidneys form tubules and are indistinguishable from wildtype littermates until at least E15.5 (Supplementary figure 3). However, conditionally mutant mice developed cystic kidneys similar to the $Wnt9b^{neo/neo}$ mice, although the onset of cystogenesis appeared to be slightly delayed. While $Wnt9b^{neo/neo}$ mice showed signs of tubule dilation as early as E15.5 (not shown) and had pronounced cysts by P1 (Figure 1e and data not shown), there were few cysts visible in KspCre;$Wnt9b^{-/flox}$ kidneys at P1 (Figure 1h). However, cysts were prevalent in KspCre;$Wnt9b^{-/flox}$ kidneys at P10 and by P30, there was little normal epithelia remaining (Figure 1i and data not shown).

To further support the hypothesis that Wnt9b had an additional role in kidney tubule morphogenesis, we performed a temporal knockout of this gene using a ubiquitously expressed, tamoxifen inducible form of Cre (CaggCreErTm)31. 15.5 days post-conception, tamoxifen was administered to $Wnt9b^{flox/flox}$ dams that had been bred to CaggCreERTm;$Wnt9b^{+/-}$ males. When tamoxifen was administered at this timepoint, the CaggCreErTm;$Wnt9b^{-/flox}$ offspring developed cysts and no mutant animals survived past P90. (Supplementary figure 4 and data not shown). However, ablation of Wnt9b after P10 (by administration of tamoxifen to 10 day old pups) did not have discernible effects on kidney morphology or function when assessed up to one year later (data not shown). These data refute the hypothesis that cyst formation is due to a defect in tubule induction or tubule maintenance. Instead, Wnt9b appears to have an additional, essential function in tubule morphogenesis.

Wnt9b acts non-autonomously to regulate tubule diameter

Wnt9b is expressed in the collecting ducts throughout embryonic development and into adult stages (Supplementary figure 1a and c and 17). To determine if Wnt9b is acting to regulate morphogenesis of the collecting ducts or if it is affecting morphogenesis of the adjacent renal vesicle derived epithelia (or both), we determined the origins of the Wnt9b mutant cysts. $Wnt9b^{neo/neo}$ and wild-type littermate kidneys were examined with markers of the proximal tubules (Lotus tetragonolobus lectin, LTL), collecting ducts (Dolichos bifloris agglutinin, DBA) and thick ascending limb of the loop of Henle (Tamm-Horsfall protein, THP) at E15.5, 18.5, P15 and P30.

Marker analysis suggested that at E15.5 and P1, cysts were present predominantly in proximal tubules (a tissue that does not express Wnt9b) and, to a lesser extent in the Wnt9b-expressing collecting ducts (Figure 2b and j and data not shown). No cysts were found in the loop of Henle or in the glomeruli at or prior to birth (Figure 2f and data not shown). However, by P15 cysts were present in all nephron segments examined (glomerulus, proximal tubule, loop of Henle and collecting duct) in approximately equal ratios (Figure 2d, h and l and data not shown). Similar results were seen in P15 KspCre;$Wnt9b^{-/flox}$ kidneys (Data not shown). These data demonstrate that after its initial role in tubule induction, Wnt9b functions non-autonomously (and possibly autonomously) to regulate the diameter of the kidney tubules.

Wnt9b is required for polarized cell division in the postnatal kidneys

To gain insights into the mechanism underlying cyst formation, Wnt9b mutant kidneys were characterized at the cellular and molecular level. Wnt9b mutant epithelia show no significant differences in their rates of proliferation or apoptosis (See supplementary notes and supplementary figure 5). However, recent studies have suggested that cell division is oriented within the plane of the tubular epithelium in postnatal kidneys and defects in orientation occur in at least five distinct models of PKD 21,32–34. The non-canonical, or planar cell polarity, branch of the Wnt pathway has been implicated in oriented cell division in gastrulating zebrafish and in worms 25,35. However, there are several examples, such as the extending Drosophila germband and the developing mouse vasculature endothelium, where oriented cell division appears to be independent of Wnt signaling 36,37. The mechanism that establishes planar polarity in the kidney epithelium remains unknown.

To assess whether Wnt9b regulated the orientation of cell division, we measured the orientation of mitotic spindles in the collecting ducts of post-natal kidneys (Supplemental figure 6d and e). To avoid complications from examining already cystic epithelia, we initially examined kidneys from the KspCre;$Wnt9b^{-/flox}$ line that develops cysts post-natally. We found that in pre-cystic, P5 KspCre;$Wnt9b^{-/flox}$ collecting ducts, cell division was not oriented within the plane of the epithelium (Figure 3b) suggesting that Wnt9b is necessary for the oriented cell divisions that occur in the post-natal kidney. The convoluted nature of the P5 proximal tubule prevented us from collecting accurate data on that segment at that timepoint.

Cell division is not oriented within the proximal tubule and collecting duct epithelium of prenatal kidneys

As cysts are present in Wnt9b$^{neo/neo}$ kidneys before birth, the mechanism for establishing tubule diameter must be active during embryogenesis. To test whether orientation of cell division played a mechanistic role in the establishment of wild type tubule diameter, we also measured the orientation of mitotic spindles in straight segments of proximal tubules and collecting ducts at E13.5 and E15.5. Surprisingly, we found that cell division was not oriented within the plane of the tubular epithelium in wild-type collecting ducts or proximal tubules at these times (Figure 3a and Supplementary figure 6a, b and data not shown). In fact, the distribution of cell divisions was not significantly different from that predicted for a completely random distribution (Figure 3a and Supplementary figure 6a, b and data not shown).

To determine when cell division becomes oriented, we examined mitotic spindles in proximal tubules and collecting ducts at early post-natal stages. We found that at P1, orientation was no longer random (from a statistical perspective) but also was not tightly oriented within the plane of the epithelium as compared to later post natal stages (Supplementary figure 6b). The distribution of mitotic angles in P1 kidneys is roughly biphasic with peaks at 30 and 60 degrees respectively (Supplementary figure 6b). There are two possible explanations for this biphasic distribution: either cell division becomes oriented centrifugally (that is from the medulla outward as development proceeds), or there is a general shift towards oriented cell divisions that occurs around the time of birth. To determine if cell divisions become oriented first in the oldest kidney tubules, we compared mitotic angles between cortical and medullary DBA-positive tubules. The distribution of mitotic angles showed a similar bi-phasic distribution in both domains supporting the idea that cell division is becoming oriented throughout the kidney at P1 (Supplementary figure 6c). As mentioned, at P5 the majority of cell divisions within the collecting duct are well-oriented, with 75% of mitotic spindles being oriented within 30 degrees of the longitudinal axis of the tubule (Figure 3b and Supplementary figure 6b). Once again, due to the convoluted structure of the P5 proximal tubule, we were not able to accurately measure orientation of cell division in this segment. However, similar to the collecting ducts, orientation of cell division in the P1 proximal tubules is no longer random indicating a trend towards oriented (Data not shown).

These data suggest that during embryonic stages, cell divisions are not oriented in the proximal tubules or collecting ducts but that they become oriented, at least within a subset of cells, around the time of birth. Therefore, oriented cell divisions cannot be playing a role in establishment of tubule diameter or in the defects seen in prenatal Wnt9b mutant kidneys. In support of this hypothesis, the orientation of cell division of Wnt9b mutant collecting ducts and proximal tubules was not significantly different from wild type (i.e. it was random) prior to birth (Figure 3a and Supplementary figure 6a).

The number of cells that make up the circumference of the kidney tubule decreases during embryogenesis

In the absence of cell loss, cell division that is not oriented within the plane of the tubular epithelium would be predicted to lead to an increase in the number of cells within the tubule wall and, in the absence of changes in cell shape or size, a concomitant increase in cross-sectional tubular diameter. To test if wildtype tubules increased the number of cells in their walls during the embryonic period, the average number of cells that make up the circumference of both proximal tubules and collecting ducts was calculated (Figure 4a–f and data not shown). Counts were taken from E13.5 (the earliest stage at which we could find both LTL and DBA positive tubules) to P1 (prior to highly oriented cell divisions). Contrary to the expectation, we found that the number of cells that make up the tubular circumference decreases by more than half from E13.5 to P1 in both collecting ducts and proximal tubules (Figure 4e and f). Importantly, the rate of cell loss during this period cannot account for this decrease (Supplementary figure 5b and d and data not shown), suggesting that some unidentified process must be driving the decrease in the number of cells making up the tubular circumference during the embryonic period.

Wnt9b mutants show defects in planar cell polarity

One process that could lead to a decrease in the number of cells within the circumference of the tubule, without affecting cell number, is convergent extension. Convergent extension describes the directed integration/intercalation of cells within an epithelium that makes the epithelium longer and narrower 26,38–43.

Convergent extension movements rely on dynamic cell shape changes and cell intercalations that are the results of reorganization of the cytoskeleton. Mediolateral elongation of cells perpendicular to the axis of extension is correlated with, and appears necessary for, intercalation of cell during convergent extension in multiple tissues 44–47. Examination of frontal sections of developing wild-type kidney tubules indicated that the majority of collecting duct cells showed polarized elongation (Figure 5a–c, g and data not shown) and that greater than 70% of elongated cells were oriented between 45 and 90 degrees (perpendicular) of the longitudinal axis of the tubule (Figure 5 b and g). Moreover, 41.3% of elongated cells were oriented within 70–90 degrees (Figure 5b and g). In contrast, collecting duct cells in $Wnt9b^{neo/neo}$ mutants showed a randomized elongation (Figure 5d–g and data not shown). Only 38% of cells in $Wnt9b^{neo/neo}$ mutants were elongated within 45–90 degrees and only 14% within 70–90 degrees (Figure 5e and g). These defects suggest that Wnt9b plays a role in establishing planar polarity of the kidney epithelium. Similar results were found in the KspCre;$Wnt9b^{-/flox}$ mutants (Figure 5h). These data suggest that Wnt9b mutant epithelia have defects in planar cell polarity that affect both cell movements and oriented cell divisions.

If defects in polarized cell orientation lead to defects in convergent extension movements, one would predict that the mutant tubules would possess a greater number of cells in their cross sectional circumference. Indeed, this was the case. $Wnt9b^{neo/neo}$ mutants had a significantly increased number of cells per tubule wall in the proximal tubules and collecting ducts at E13.5, 15.5, 17.5 and P1 (Figure 4e and f and data not shown). Cell size however

did not appear to be affected (data not shown). It is important to note that the cellular numbers calculated for later stage (E15.5-P1) mutants are most likely an underestimate of true values. In order to assure that only epithelial cross sections were evaluated, we did not analyze tubules that varied significantly from being perfect circles (see Materials and Methods). At later stages, due to drastically increased diameter, most mutant tubules were grossly misshapened and were excluded from the analysis. Therefore, the mutant tubules assessed are the most "wildtype" examples leading to an underestimate of the true number of cells per mutant tubule wall.

Wnt9b signals through a non-canonical pathway to regulate tubule elongation

Although previous studies suggested that Wnt9b signaled through the canonical/β–catenin dependent signal transduction branch during kidney tubule induction 17,18, this pathway appeared to be unaffected in the cystic mutants (See supplementary notes and Figure 6a–c). These data suggest that Wnt9b signals through one of the non-canonical pathways to regulate tubule diameter. As the PCP branch of this pathway has previously been implicated in cell orientation and convergent extension movements, we sought to determine if its activity was affected in Wnt9b mutants. Although there is no established molecular readout of PCP in vertebrates, it has been shown that signaling through this pathway can activate the Rho-GTPases and Jun kinase (Jnk) 48–50. Activated (GTP bound) levels of Rho (but not Cdc42 or Rac) were significantly decreased relative to total Rho levels in mutants (Figure 6d and data not shown). Further, we found a significant decrease in the level of phosphorylated Jnk2 (relative to total Jnk2) in P1 Wnt9b mutant kidneys (Figure 6d). These data support the hypothesis that Wnt9b signals through the non-canonical/PCP pathway to regulate convergent extension and oriented cell division during kidney tubule morphogenesis.

Discussion

In this study, we demonstrate that, in addition to its initial role in renal vesicle formation, Wnt9b plays a later role in renal tubule morphogenesis. Mice carrying a hypomorphic mutation of Wnt9b or mice that have had a floxed allele of Wnt9b deleted with either KspCre or the tamoxifen inducible CaggCreErTm;Wnt9b$^{-/flox}$ develop cystic kidneys. Cystogenesis does not appear to be caused by increased cell numbers as we have not detected differences in the rates of cell proliferation or apoptosis in mutant epithelia either prior to or concurrent with cyst formation. Instead, we hypothesize that cyst formation is the result of defects in planar cell polarity. We show that cells within the epithelial tubule are elongated perpendicular to the proximal/distal axis of the tubule and that this process is dependent on Wnt9b. We hypothesize that proper cell orientation is required for convergent extension movements and oriented cell divisions. Although cells within the normal collecting ducts and proximal tubules of embryonic kidneys divide in a random orientation, the number of cells composing the wall of the tubule decreases during the embryonic period. We hypothesize that convergent extension movements drive the number of cells within the circumference (or wall) of a tubule to decrease as the tubule elongates. This process, at least in part, establishes the tubule diameter and contributes to tubule length. Once the tubule diameter is established, cell division becomes oriented parallel to the proximal/distal axis to ensure that the kidney tubules continue to elongate while they maintain their diameter. Our

data suggest that Wnt9b plays essential roles in both of these processes, perhaps by mediating cell orientation.

In stark contrast to its β–catenin dependent/canonical role during tubule induction17,18, we have shown that the role of Wnt9b in establishing and maintaining tubule diameter is β–catenin independent. Instead, Wnt9b appears to signal through the non-canonical Rho/Jnk pathway during tubule morphogenesis. Interestingly, recent studies showed that attenuation of Rho kinase led to shorter, wider tubules in cultured kidneys51,52, a phenotype that may reflect attenuation of Wnt9b signaling. Our data support a hypothesis where Wnt pathway usage is not determined by the individual ligand but instead by the cellular environment in which the signal is received. Depending on the cell type, Wnt9b can signal through both pathways within the same organ system.

Several factors involved in cystic kidney diseases are localized to, and/or are necessary for the function of, the apical mono-cilia 32,53–64. In addition, recent studies suggest that the primary cilium may play a role in inhibiting canonical Wnt signaling (perhaps promoting non-canonical Wnt signaling) in early mouse and zebrafish embryos 65,66. A simple model for Wnt pathway usage in the kidney is that the cilia and/or ciliary factors block canonical signaling by Wnt9b and promote non-canonical signaling. Indeed, we see no defects in the expression or localization of several ciliary factors such as Pc-1 and Pc-2 (factors involved in the progression of human autosomal dominant PKD) 61,67 and inversin (Inv) mRNA (the ortholog of the gene mutated in Nephronophthisis type II)60 in Wnt9b mutants nor is Wnt9b mRNA expression affected in $Inv^{-/-}$ 68 or $Pkd1^{-/-}$ 67 mice (data not shown).

Although this study has revealed a great deal about the mechanisms that regulate tubule diameter, several questions remain unanswered. One such question is why Wnt9b cysts are primarily restricted to the cortex of the kidney? There are several possible answers. The simplest is that another molecule compensates for Wnt9b in the medullary region. Several Wnts, including Wnt5a, Wnt7b, Wnt4 and Wnt11, are expressed in the medullary region of both wild type and Wnt9b mutant kidneys (69 and Karner and Carroll, unpublished observations) and any one of these factors may compensate for loss of Wnt9b. Alternatively, there may be a parallel, Wnt independent, signaling pathway that regulates PCP in the medulla. A recent study showed that mice lacking the PCP determinant Fat4 developed kidney cysts primarily within the medullary region 34. Compensation by either another Wnt or Fat4 would explain the paucity of medullary cysts in Wnt9b mutants. However, it is important to note that we do observe increased numbers of cells within the circumference of the Wnt9b mutant collecting ducts as well as defects in cell orientation during embryonic stages but do not observe cysts in this nephron segment until post-natal stages. Similar findings were observed by Yu et al. 69 suggesting that other processes, such as defects in fluid secretion or cellular growth (hypertrophy) most likely contribute to cyst formation.

Another question raised by these findings is how Wnt9b, produced by the collecting ducts, affects planar cell polarity in the relatively distant proximal tubules? The simplest hypothesis is that Wnt9b, secreted from the collecting ducts, travels vertically through the stroma to polarize the epithelia. However, it is formally possible that Wnt9b travels through the lumen or through the plane of the epithelium (transcytosis) to regulate morphogenesis.

This question is complicated by the fact that we do not know the cell type that is the target of Wnt9b nor do we know at precisely what step during tubule morphogenesis Wnt9b acts, as evidenced by the disparate onset of cystogenesis in KspCre;Wnt9b$^{-/flox}$ and CaggCreErTm;Wnt9b$^{-/flox}$ mutants. Our model is that Wnt9b signals relatively late or continuously during tubule morphogenesis. However, it is possible that it Wnt9b establishes polarity early on in the process of tubule formation, acting on the metanephric mesenchyme or renal vesicles. Finally, it is possible that Wnt9b does not signal directly to the epithelial cells, instead directly signaling to the intervening stroma, which secondarily affects morphogenesis. Determining which of these mechanisms is utilized will be facilitated by the identification of molecular targets of Wnt9b.

A final question that remains is whether Wnt9b contributes to human forms of PKD. Wnt9b continues to be expressed in the adult kidney suggesting that it may play a role in kidney maintenance and/or repair and that improper regulation of this molecule in adults leads to cystogenesis. For instance, improper activation of canonical Wnt9b activity (or failure to divert Wnt9b signaling through the non-canonical branch) in adult kidneys due to loss of ciliary signaling may play a causal role in cystogenesis. Determining if this is the case will require simultaneous ablation of Wnt9b in kidneys that lack intact ciliary signaling or in injured kidneys.

In sum, our findings show that Wnt9b, produced by the kidney collecting ducts, non-autonomously regulates morphogenesis of the developing kidney tubules. We suggest that Wnt9b is required for PCP and the PCP dependent cellular processes convergent extension and oriented cell division. These processes are in turn required to establish and maintain the tubular diameter and length during the embryonic period but are dispensible in healthy, differentiated tubules. A better grasp of the regulation and downstream targets of Wnt9b will significantly impact our understanding of epithelial tubule morphogenesis and the treatment of polycystic kidney disease.

Methods

Generation of Wnt9b mutant mice and genotyping

The Wnt9b^{-} and Wnt9b^{neo} alleles were previously described 17. The neomycin cassette in the Wnt9b^{neo} mice was flanked by flp recombinase target sites (frt). To generate the Wnt9b^{flox} mice, Wnt9b$^{neo/+}$ animals were crossed to mice carrying a ubiquitously expressed flippase gene. Removal of the neomycin cassette was confirmed by Southern blot. Males and females that had had the neomycin cassette excised were crossed to each to generate (Wnt9b$^{flox/flox}$) animals. These mice were maintained as a homozygous line. To generate the conditional null kidneys, KspCre;Wnt9b$^{+/-}$ males were crossed to Wnt9b$^{flox/flox}$ females. Noon of the day of vaginal plugging was considered E0.5.

Genotyping of mice was performed by digesting a 0.5 cm piece of tail in tail lysis buffer (Viagen) at 55 degrees overnight. The floxed and null alleles were amplified in a single reaction using the conditions previously described 17. The null allele generates a 500 bp band, the flox allele a 240 base pair band and the wild-type allele a 200 bp band. The *KspCre* and *CaggCreERTM* alleles where amplified using the described in the

supplementary table to give a 400 base pair band using the conditions previously described. The β–catenin exon3flox mice were provided by Mark Taketo 70. Using the primers listed in the supplementary table and a 55 ° extension, the wild type allele gives a 291 base pair band while the exon 3 floxed allele gives a 400 base pair band.

Immunohistochemistry

Specimens were fixed in 4% paraformaldehyde in PBS (EMS) for 16 hours at 4 degrees C, washed 3 times with PBS and cryoprotected in 30% sucrose for 16 hours at 4 degrees C. Specimens were then embedded in OCT and cryosectioned at the thicknesses indicated. Immunohistochemistry was performed as previously described 71. Specimens were examined by scanning laser confocal microscopy (Zeiss LSM-510). Sections were stained with the following lectins or antibodies: *Dolichos bifloris* lectin (DBA, Biotinylated, 1:500 Vector Laboratories), *Lotus Tetragonolobus* lectin (LTL, Biotinylated, 1:500 Vector Laboratories), anti-Laminin (Rabbit polyclonal, 1:300 Sigma), anti-Tamm-Horsfall protein (Rabbit, 1:300 Biomedical Technologies), anti-E-cadherin (Rat, 1:500 Zymed), anti-Ki67 (Rabbit, 1:800 Novocastra), anti-cleaved caspase-3 (Rabbit, 1:300 Promega), anti-GFP (Rabbit, 1:1000 Abcam), anti aPKC (Rabbit, 1:500 Santa Cruz), and Sytox Green (1:5000, Invitrogen).

Western blotting

Wild type and Wnt9b$^{neo/neo}$ (P1) kidneys were homogenized in a medium containing 20mM Hepes (Ph 7.4), 10mM NaCl, 1.5mM MgCl2, 20% glycerol, 0.1%Triton X-100, 1Mm DTT, 1.5mM sodium orthovanadate and protease inhibitor mix (Complete Mini, one protease inhibitor cocktail tablet per 20 ml of medium. Roche Molecular Biochemicals, Catalog: 04693124001) in a dounce homogenizer by giving 40 strokes. The lysate was centrifuged at 3400 rpm for 3 min in 4°C to separate the cytosolic and nuclear fractions. Supernatant was used as the cytosolic fraction. Protein concentration was estimated by the method of Bradford.

Protein (50ug) was resolved on 10% polyacrylamide gel and subjected to immunoblot analysis using the respective antibodies. GAPDH was used as a loading control. Antibodies against pJnk1/2 (1:500 dilution, Biosource, Catalog: 44–682G), total Jnk2 (1:1000 dilution, Cell signaling Technology, Catalog: 4672), dephosphorylated β–Catenin (1:1000 dilution, Upstate Cell signaling solutions, catalog: 05–601) and GAPDH (1:3000 dilution, Santa Cruz Biotechnology, Catalog: sc25778) were used to detect the respective protein levels in wild-type and Wnt9b$^{neo/neo}$ cytosolic fractions. The immunoblots were blocked for one hour at room temperature in 5% Non-fat dry milk (1× TBS, 0·05% Tween) followed by an overnight incubation at 4°C in their respective diluted primary antibody solutions. Membranes were then washed three times using TBS/Tween 0×05% (5 min/15 ml) and further incubated with the secondary antibody, HRP goat anti rabbit (Invitrogen, Catalog: G21234) in 5% Non-fat dry milk (1×TBS/Tween 0·05%) for 1 h at room temperature (1:5000 to detect pJnk1/2, 1:2000 to detect total Jnk2 and 1:10,000 to detect GAPDH levels). Dephosphorylated β–catenin was detected using HRP Goat anti mouse (1:5000, Pierce, catalog: 1858413) using the same conditions as described above. All the blots were developed using the Pierce Super signal West Femto maximum sensitivity substrate kit.

Quantification of the proteins levels was done using Image J software. Each experiment was done a minimum of three times with at least two independently prepared protein samples.

Rho Pulldown

Activated Rho was pulled down from Wild type and Wnt9b$^{neo/neo}$ P1 kidneys using EZ-Detect™ Rho Activation Kit with slight modification to the manufacturer's protocol (Pierce, Catalog: 89854). The kidneys were homogenized in the lysis buffer provided in the kit with the addition of protease inhibitor mix (Complete Mini, one protease inhibitor cocktail tablet per 10 ml of medium, Roche Molecular Biochemicals, Catalog: 04693124001) in a dounce homogenizer by giving 10–15 strokes. The lysate was centrifuged at 14,000 rpm at 4°C for 10 minutes. Supernatant was separated and used for the assay. 1mg of protein was used for each pull down assay. In vitro control treatments were done by the addition of GTP (positive control) or GDP (negative control) to activate or inactivate Rho respectively.

Protein was resolved on 12% polyacrylamide gel and subjected to immunoblot analysis using anti-Rho antibody. The immunoblots were blocked in TBS containing 3% BSA at room temperature for 2 hrs followed by an overnight incubation in primary antibody solution (1:500 dilution in 3% BSA in TBS/Tween-0.05%) at 4°C. Membranes were washed three times using 15 ml of TBS/Tween-0.05% (5 min each wash) and further incubated with the secondary antibody, HRP goat anti Mouse (Invitrogen, Catalog: G21040) in 5% NFDM (1×TBS/Tween 0.05%) for 1 h at room temperature (1:10000 dilution). Immunoblots were developed using Pierce Super signal West Femto maximum sensitivity substrate kit.

In situ Hybridization

In situ hybridization was performed on 30 or 16 uM cryosectioned kidneys as previously described 17. Sections labeled with DBA lectin where washed 3 times in PBS after the color reaction, fixed in 4% paraformaldehyde in PBS (EMS) for 1 hour at room temperature, washed 3 times with PBS and processed for immunohistochemistry as described previously 71. Kidneys stained for X-gal were fixed (1% PFA, 0.2% gluteraldehyde in PBS) for 1 hour, washed 3 times with 0.02%NP-40/PBS, stained (5mM K3Fe(CN)6, 5mM K4Fe(CN)6, 2mM MgCl2, 0.01% NaDeoxycholate, 0.02% NP-40, 1mg/ml X-gal) for up two 2 hours at 37 degrees. Staining was stopped by washing in PBS followed by fixation in 4% PFA + 0.2% gluteraldehyde for 30 minutes. Samples were then processed for wholemount *in situ* hybridization as previously 17. Sections to be stained for X-gal were fixed as for whole mount staining and processed for cryosectioning as described above. 14 uM sections were washed 3 times with PBS and stained for beta-galactosidase activity for a maximum of 1 hour at 37 degrees C. Staining was stopped by washing 3 times for 10 minutes in PBS followed by a 10 minute fixation in 4% PFA before proceeding to section *in situ* hybridization.

Tubule diameter counts

To quantitate the number of cells making up the cross-sectional wall of individual tubules, 10uM kidney sections were stained with segment specific markers (DBA or LTL), antibodies to the extracellular matrix protein laminin and the nuclear marker Dapi. For the

collecting ducts, we excluded the cortical most epithelia to avoid branching tubules. To assure that only cross sections were being analyzed, the diameter of the tubule was measured at two intersecting lines that were perpendicular to each other. If the two measured diameters varied by more than 10% (making the shape of tubule more of an oval than a circle), the section was assumed to be frontal and therefore excluded from analysis. If a tubule was considered to be transverse, the number of nuclei in the tubular cross section was averaged. This was performed for both the collecting ducts and the proximal tubules at multiple embryonic and postnatal timepoints (E13.5, 15.5, 17.5 and P1). Statistical differences between wild-type and mutants were assessed by Student's T-test.

Measuring the orientation of cell division

To evaluate the orientation of cell division we utilized a protocol similar to that described by Fischer *et al* with slight modification 21. 50 uM thick E13.5, 15.5, P1 and P5 kidney sections were labeled with an anti-laminin antibody, a tubule specific marker (DBA or LTL) and Sytox green. For the collecting ducts, we excluded the cortical most epithelia to avoid branching tubules. Labeled tubules containing anaphase nuclei where identified and a Z-stack was taken using the Zeiss LSM-510. These images where reconstructed using the Imaris software and Cartesian coordinates where assigned for the mitotic spindles and basal lamina of the tubule (Supplemental Figure 5C and D). The angle between the resulting vectors was determined according to 21. The randomness of cell division was determined by the Kolmogorov-Smirnov Goodness of Fit Test.

Measurement of cell elongation and orientation

To determine if cells were elongated, sections of E15.5 kidneys were stained with DBA, E-cadherin and aPKC. The cortical most epithelia were excluded to avoid branching tubules. Z-stacks were captured and sections were identified that were frontal through the collecting duct and that fell one frame below (basal to) the aPKC staining. Using Image ProPlus software, two roughly parallel lines were drawn on opposite sides of every cell in the image where E-cadherin staining outlined the entire cell (Cells on the edges that had discontinuous E-cadherin staining were not measured). The software then calculated the average distance between those two lines and assigned a length to width ratio for each individual cell, with the length being the longer of the two sides. Cells that possessed a length to width ratio of greater than 1.2 were considered elongated. To measure the orientation of elongated cells, a vector was assigned for the elongated axis of the cell and the elongated axis of the tubule. The angle between these two vectors was determined using Image ProPlus software. The percentage of total cells that fell within each 10° bin was calculated. Statistical analysis for the wild-type and mutant populations was performed according to the Mann-Whitney U test.

Supplementary Material

Refer to Web version on PubMed Central for supplementary material.

Acknowledgements

We would like to thank Ondine Cleaver for reading and commenting on this manuscript, Leon Avery for help with statistical analysis, Jing Zhou for providing us with antibodies to Pc-1 and Pc-2 and the Pkd1 mutant kidneys, Olga

Caballo for providing us with the Inv mutant kidneys, Bryan Adams, Erin Small, John Shelton and the Molecular Pathology Core for technical assistance and Leighton James and Maile Princena for the urine albumin studies. This work was supported by grants from the American Society for Nephrology, the American Heart Association (0730236N), the Polycystic Kidney Disease Research Foundation, the UAB ARPKD Center (5P30DK07403802) and the N.I.H. (1R01DK080004) to T.J.C. The work was also supported by the UT Southwestern O'Brien Kidney Research Core Center (NIH P30DK079328). JBW was supported by grants from the NIGMS, the March of Dimes and the Burroughs Wellcome Fund.

References for Methods

70. Harada N, et al. Intestinal polyposis in mice with a dominant stable mutation of the beta-catenin gene. Embo J. 1999; 18:5931–5942. [PubMed: 10545105]

71. Marose TD, Merkel CE, McMahon AP, Carroll TJ. Beta-catenin is necessary to keep cells of ureteric bud/Wolffian duct epithelium in a precursor state. Dev Biol. 2008; 314:112–126. [PubMed: 18177851]

References

1. Schedl A. Renal abnormalities and their developmental origin. Nat Rev Genet. 2007; 8:791–802. [PubMed: 17878895]

2. Torres VE, Harris PC, Pirson Y. Autosomal dominant polycystic kidney disease. Lancet. 2007; 369:1287–1301. [PubMed: 17434405]

3. Ibraghimov-Beskrovnaya O. Targeting dysregulated cell cycle and apoptosis for polycystic kidney disease therapy. Cell Cycle. 2007; 6:776–779. [PubMed: 17377490]

4. Araujo SJ, Aslam H, Tear G, Casanova J. mummy/cystic encodes an enzyme required for chitin and glycan synthesis, involved in trachea, embryonic cuticle and CNS development--analysis of its role in Drosophila tracheal morphogenesis. Dev Biol. 2005; 288:179–193. [PubMed: 16277981]

5. Jayaram SA, et al. COPI vesicle transport is a common requirement for tube expansion in Drosophila. PLoS ONE. 2008; 3:e1964. [PubMed: 18398480]

6. Tsarouhas V, et al. Sequential pulses of apical epithelial secretion and endocytosis drive airway maturation in Drosophila. Dev Cell. 2007; 13:214–225. [PubMed: 17681133]

7. Wang S, et al. Septate-junction-dependent luminal deposition of chitin deacetylases restricts tube elongation in the Drosophila trachea. Curr Biol. 2006; 16:180–185. [PubMed: 16431370]

8. Hemphala J, Uv A, Cantera R, Bray S, Samakovlis C. Grainy head controls apical membrane growth and tube elongation in response to Branchless/FGF signalling. Development. 2003; 130:249–258. [PubMed: 12466193]

9. Jung AC, Ribeiro C, Michaut L, Certa U, Affolter M. Polychaetoid/ZO-1 is required for cell specification and rearrangement during Drosophila tracheal morphogenesis. Curr Biol. 2006; 16:1224–1231. [PubMed: 16782014]

10. Luschnig S, Batz T, Armbruster K, Krasnow MA. serpentine and vermiform encode matrix proteins with chitin binding and deacetylation domains that limit tracheal tube length in Drosophila. Curr Biol. 2006; 16:186–194. [PubMed: 16431371]

11. Lubarsky B, Krasnow MA. Tube morphogenesis: making and shaping biological tubes. Cell. 2003; 112:19–28. [PubMed: 12526790]

12. Nishimura M, Inoue Y, Hayashi S. A wave of EGFR signaling determines cell alignment and intercalation in the Drosophila tracheal placode. Development. 2007; 134:4273–4282. [PubMed: 17978004]

13. Paul SM, Palladino MJ, Beitel GJ. A pump-independent function of the Na,K-ATPase is required for epithelial junction function and tracheal tube-size control. Development. 2007; 134:147–155. [PubMed: 17164420]

14. Wu VM, Beitel GJ. A junctional problem of apical proportions: epithelial tube-size control by septate junctions in the Drosophila tracheal system. Curr Opin Cell Biol. 2004; 16:493–499. [PubMed: 15363798]

15. Tong X, Buechner M. CRIP homologues maintain apical cytoskeleton to regulate tubule size in C. elegans. Dev Biol. 2008; 317:225–233. [PubMed: 18384766]

16. Merkel CE, Karner CM, Carroll TJ. Molecular regulation of kidney development: is the answer blowing in the Wnt? Pediatr Nephrol. 2007; 22:1825–1838. [PubMed: 17554566]
17. Carroll TJ, Park JS, Hayashi S, Majumdar A, McMahon AP. Wnt9b plays a central role in the regulation of mesenchymal to epithelial transitions underlying organogenesis of the mammalian urogenital system. Dev Cell. 2005; 9:283–292. [PubMed: 16054034]
18. Park JS, Valerius MT, McMahon AP. Wnt/beta-catenin signaling regulates nephron induction during mouse kidney development. Development. 2007; 134:2533–2539. [PubMed: 17537789]
19. Saadi-Kheddouci S, et al. Early development of polycystic kidney disease in transgenic mice expressing an activated mutant of the beta-catenin gene. Oncogene. 2001; 20:5972–5981. [PubMed: 11593404]
20. Benzing T, Simons M, Walz G. Wnt signaling in polycystic kidney disease. J Am Soc Nephrol. 2007; 18:1389–1398. [PubMed: 17429050]
21. Fischer E, et al. Defective planar cell polarity in polycystic kidney disease. Nat Genet. 2006; 38:21–23. [PubMed: 16341222]
22. Karner C, Wharton KA Jr, Carroll TJ. Planar cell polarity and vertebrate organogenesis. Semin Cell Dev Biol. 2006; 17:194–203. [PubMed: 16839790]
23. Klingensmith J, Nusse R, Perrimon N. The Drosophila segment polarity gene dishevelled encodes a novel protein required for response to the wingless signal. Genes Dev. 1994; 8:118–130. [PubMed: 8288125]
24. Vinson CR, Conover S, Adler PN. A Drosophila tissue polarity locus encodes a protein containing seven potential transmembrane domains. Nature. 1989; 338:263–264. [PubMed: 2493583]
25. Goldstein B, Takeshita H, Mizumoto K, Sawa H. Wnt signals can function as positional cues in establishing cell polarity. Dev Cell. 2006; 10:391–396. [PubMed: 16516841]
26. Heisenberg CP, et al. Silberblick/Wnt11 mediates convergent extension movements during zebrafish gastrulation. Nature. 2000; 405:76–81. [PubMed: 10811221]
27. Tada M, Smith JC. Xwnt11 is a target of Xenopus Brachyury: regulation of gastrulation movements via Dishevelled, but not through the canonical Wnt pathway. Development. 2000; 127:2227–2238. [PubMed: 10769246]
28. Wehrli M, et al. arrow encodes an LDL-receptor-related protein essential for Wingless signalling. Nature. 2000; 407:527–530. [PubMed: 11029006]
29. Shao X, Somlo S, Igarashi P. Epithelial-specific Cre/lox recombination in the developing kidney and genitourinary tract. J Am Soc Nephrol. 2002; 13:1837–1846. [PubMed: 12089379]
30. Thomson RB, Aronson PS. Immunolocalization of Ksp-cadherin in the adult and developing rabbit kidney. Am J Physiol. 1999; 277:F146–F156. [PubMed: 10409308]
31. Hayashi S, McMahon AP. Efficient recombination in diverse tissues by a tamoxifen-inducible form of Cre: a tool for temporally regulated gene activation/inactivation in the mouse. Dev Biol. 2002; 244:305–318. [PubMed: 11944939]
32. Jonassen JA, San Agustin J, Follit JA, Pazour GJ. Deletion of IFT20 in the mouse kidney causes misorientation of the mitotic spindle and cystic kidney disease. J Cell Biol. 2008; 183:377–384. [PubMed: 18981227]
33. Patel V, et al. Acute kidney injury and aberrant planar cell polarity induce cyst formation in mice lacking renal cilia. Hum Mol Genet. 2008
34. Saburi S, et al. Loss of Fat4 disrupts PCP signaling and oriented cell division and leads to cystic kidney disease. Nat Genet. 2008; 40:1010–1015. [PubMed: 18604206]
35. Gong Y, Mo C, Fraser SE. Planar cell polarity signalling controls cell division orientation during zebrafish gastrulation. Nature. 2004; 430:689–693. [PubMed: 15254551]
36. da Silva SM, Vincent JP. Oriented cell divisions in the extending germband of Drosophila. Development. 2007; 134:3049–3054. [PubMed: 17652351]
37. Zeng G, et al. Orientation of endothelial cell division is regulated by VEGF signaling during blood vessel formation. Blood. 2007; 109:1345–1352. [PubMed: 17068148]
38. Wang J, et al. Regulation of polarized extension and planar cell polarity in the cochlea by the vertebrate PCP pathway. Nat Genet. 2005; 37:980–985. [PubMed: 16116426]

39. Wallingford JB, Vogeli KM, Harland RM. Regulation of convergent extension in Xenopus by Wnt5a and Frizzled-8 is independent of the canonical Wnt pathway. Int J Dev Biol. 2001; 45:225–227. [PubMed: 11291850]
40. Torban E, Wang HJ, Groulx N, Gros P. Independent mutations in mouse Vangl2 that cause neural tube defects in looptail mice impair interaction with members of the Dishevelled family. J Biol Chem. 2004; 279:52703–52713. [PubMed: 15456783]
41. Djiane A, Riou J, Umbhauer M, Boucaut J, Shi D. Role of frizzled 7 in the regulation of convergent extension movements during gastrulation in Xenopus laevis. Development. 2000; 127:3091–3100. [PubMed: 10862746]
42. Goto T, Davidson L, Asashima M, Keller R. Planar cell polarity genes regulate polarized extracellular matrix deposition during frog gastrulation. Curr Biol. 2005; 15:787–793. [PubMed: 15854914]
43. Goto T, Keller R. The planar cell polarity gene strabismus regulates convergence and extension and neural fold closure in Xenopus. Dev Biol. 2002; 247:165–181. [PubMed: 12074560]
44. Marlow F, Topczewski J, Sepich D, Solnica-Krezel L. Zebrafish Rho kinase 2 acts downstream of Wnt11 to mediate cell polarity and effective convergence and extension movements. Curr Biol. 2002; 12:876–884. [PubMed: 12062050]
45. Concha ML, Adams RJ. Oriented cell divisions and cellular morphogenesis in the zebrafish gastrula and neurula: a time-lapse analysis. Development. 1998; 125:983–994. [PubMed: 9463345]
46. Wallingford JB, et al. Dishevelled controls cell polarity during Xenopus gastrulation. Nature. 2000; 405:81–85. [PubMed: 10811222]
47. Shih J, Keller R. Cell motility driving mediolateral intercalation in explants of Xenopus laevis. Development. 1992; 116:901–914. [PubMed: 1295743]
48. Habas R, Dawid IB, He X. Coactivation of Rac and Rho by Wnt/Frizzled signaling is required for vertebrate gastrulation. Genes Dev. 2003; 17:295–309. [PubMed: 12533515]
49. Strutt DI, Weber U, Mlodzik M. The role of RhoA in tissue polarity and Frizzled signalling. Nature. 1997; 387:292–295. [PubMed: 9153394]
50. Boutros M, Paricio N, Strutt DI, Mlodzik M. Dishevelled activates JNK and discriminates between JNK pathways in planar polarity and wingless signaling. Cell. 1998; 94:109–118. [PubMed: 9674432]
51. Michael L, Sweeney DE, Davies JA. A role for microfilament-based contraction in branching morphogenesis of the ureteric bud. Kidney Int. 2005; 68:2010–2018. [PubMed: 16221201]
52. Meyer TN, et al. Rho kinase acts at separate steps in ureteric bud and metanephric mesenchyme morphogenesis during kidney development. Differentiation. 2006; 74:638–647. [PubMed: 17177859]
53. Yoder BK, et al. Polaris, a protein disrupted in orpk mutant mice, is required for assembly of renal cilium. Am J Physiol Renal Physiol. 2002; 282:F541–F552. [PubMed: 11832437]
54. Yoder BK, Hou X, Guay-Woodford LM. The polycystic kidney disease proteins, polycystin-1, polycystin-2, polaris, and cystin, are co-localized in renal cilia. J Am Soc Nephrol. 2002; 13:2508–2516. [PubMed: 12239239]
55. Watanabe D, et al. The left-right determinant Inversin is a component of node monocilia and other 9+0 cilia. Development. 2003; 130:1725–1734. [PubMed: 12642479]
56. Ward CJ, et al. Cellular and subcellular localization of the ARPKD protein; fibrocystin is expressed on primary cilia. Hum Mol Genet. 2003; 12:2703–2710. [PubMed: 12925574]
57. Sun Z, et al. A genetic screen in zebrafish identifies cilia genes as a principal cause of cystic kidney. Development. 2004; 131:4085–4093. [PubMed: 15269167]
58. Baker SA, Freeman K, Luby-Phelps K, Pazour GJ, Besharse JC. IFT20 links kinesin II with a mammalian intraflagellar transport complex that is conserved in motile flagella and sensory cilia. J Biol Chem. 2003; 278:34211–34218. [PubMed: 12821668]
59. Pazour GJ, San Agustin JT, Follit JA, Rosenbaum JL, Witman GB. Polycystin-2 localizes to kidney cilia and the ciliary level is elevated in orpk mice with polycystic kidney disease. Curr Biol. 2002; 12:R378–R380. [PubMed: 12062067]

60. Otto EA, et al. Mutations in INVS encoding inversin cause nephronophthisis type 2, linking renal cystic disease to the function of primary cilia and left-right axis determination. Nat Genet. 2003; 34:413–420. [PubMed: 12872123]
61. Nauli SM, et al. Polycystins 1 and 2 mediate mechanosensation in the primary cilium of kidney cells. Nat Genet. 2003; 33:129–137. [PubMed: 12514735]
62. Menezes LF, et al. Polyductin, the PKHD1 gene product, comprises isoforms expressed in plasma membrane, primary cilium, and cytoplasm. Kidney Int. 2004; 66:1345–1355. [PubMed: 15458427]
63. Hou X, et al. Cystin, a novel cilia-associated protein, is disrupted in the cpk mouse model of polycystic kidney disease. J Clin Invest. 2002; 109:533–540. [PubMed: 11854326]
64. Lin F, et al. Kidney-specific inactivation of the KIF3A subunit of kinesin-II inhibits renal ciliogenesis and produces polycystic kidney disease. Proc Natl Acad Sci U S A. 2003; 100:5286–5291. [PubMed: 12672950]
65. Corbit KC, et al. Kif3a constrains beta-catenin-dependent Wnt signalling through dual ciliary and non-ciliary mechanisms. Nat Cell Biol. 2008; 10:70–76. [PubMed: 18084282]
66. Gerdes JM, et al. Disruption of the basal body compromises proteasomal function and perturbs intracellular Wnt response. Nat Genet. 2007; 39:1350–1360. [PubMed: 17906624]
67. Lu W, et al. Perinatal lethality with kidney and pancreas defects in mice with a targetted Pkd1 mutation. Nat Genet. 1997; 17:179–181. [PubMed: 9326937]
68. Simons M, et al. Inversin, the gene product mutated in nephronophthisis type II, functions as a molecular switch between Wnt signaling pathways. Nat Genet. 2005; 37:537–543. [PubMed: 15852005]
69. Yu J, et al. A Wnt7b-dependent pathway regulates the orientation of epithelial cell division and establishes the cortico-medullary axis of the mammalian kidney. Development. 2009; 136:161–171. [PubMed: 19060336]

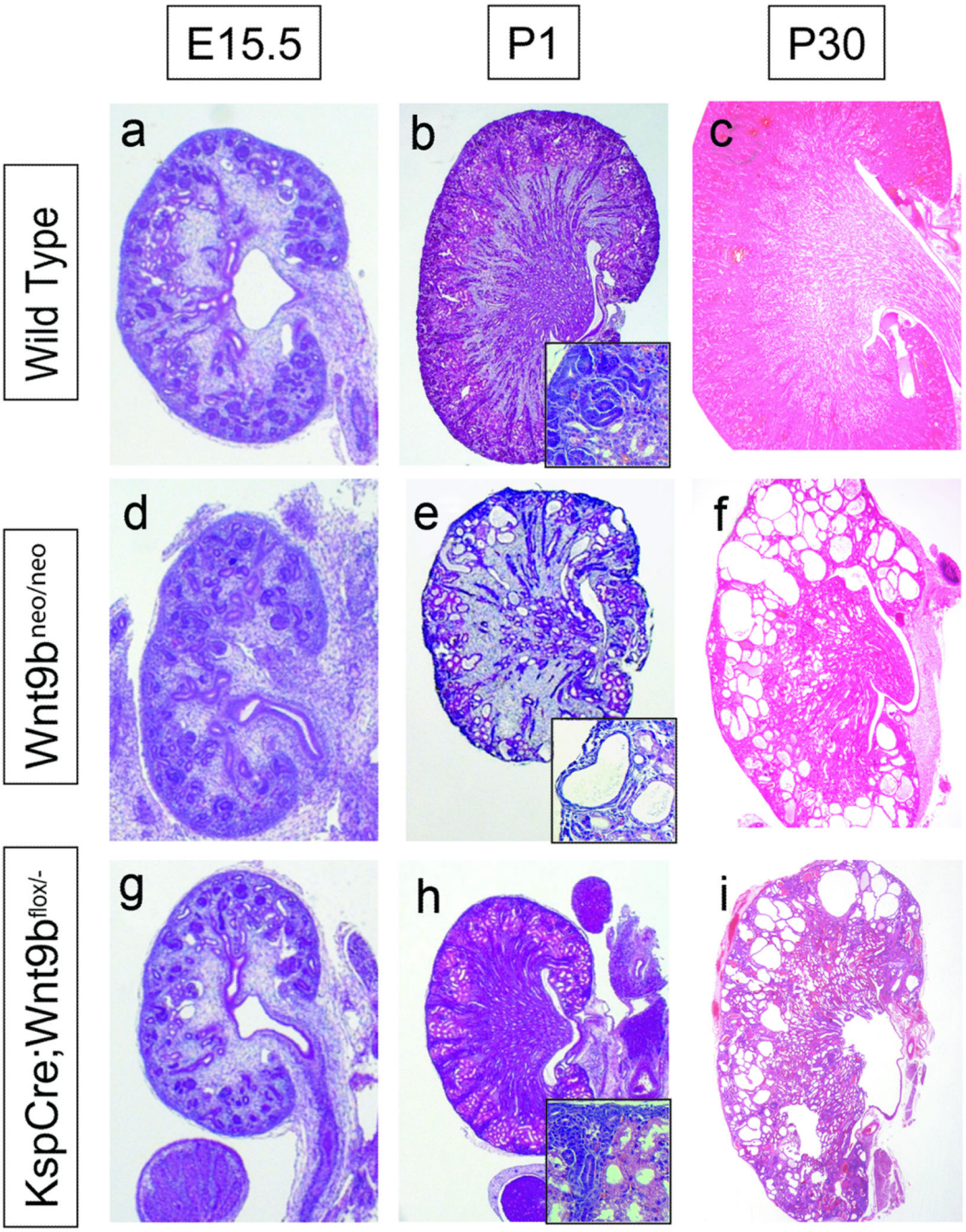

Figure 1. Defects in Wnt9b signaling results in cyst formation

H&E sections of wild type (a–c), Wnt9b$^{neo/neo}$ (d–f), and KspCre;Wnt9b$^{flox/-}$ (g–i) kidneys at embryonic day 15.5 (a,d and g), postnatal day 1 (b, e and h) or postnatal day 30 (c, f and i). Wnt9b mutant kidneys appear normal at E15.5 (compare d and g to a) but are smaller at birth (compare e and h to b). Wnt9b$^{cneo/cneo}$ kidneys also show signs of cystic dysplasia at P1 (e). At one month of age mutant kidneys are slightly smaller and severely cystic compared to wild type kidneys (compare f and i to c). Insets in B, E and H show high magnification images of cortical epithelia.

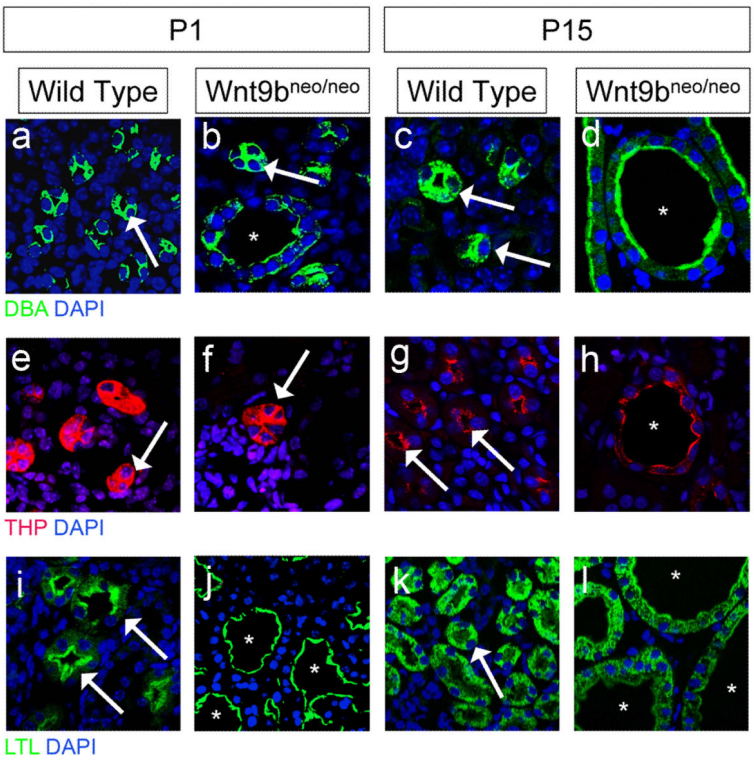

Figure 2. Characterization of cyst origin in Wnt9b$^{neo/neo}$ kidneys

Sections of P1 (a, b, e, f, i, j) and P15 (c, d, g, h, k, l) kidneys stained with the collecting duct specific marker Dolichos biflorus agglutinin (DBA) in a–d, the loop of Henle marker Tamm Horsfall protein (THP) in e–h, and the proximal tubule marker Lotus tetragolonobus lectin (LTL) in i–l. In all panels arrows denote normal tubules and asterisks denote cystic tubules. At birth, cysts are found primarily in the proximal tubules (compare i to j). Cysts are also found in the collecting ducts although the majority of DBA positive epithelia appear normal (see arrows in b). Cysts were not observed in the loop of Henle at birth (compare e to f). By P15 cysts are present in all segments of the nephron (compare c to b, g to h, and k to l). Nuclei were counterstained with DAPI (blue).

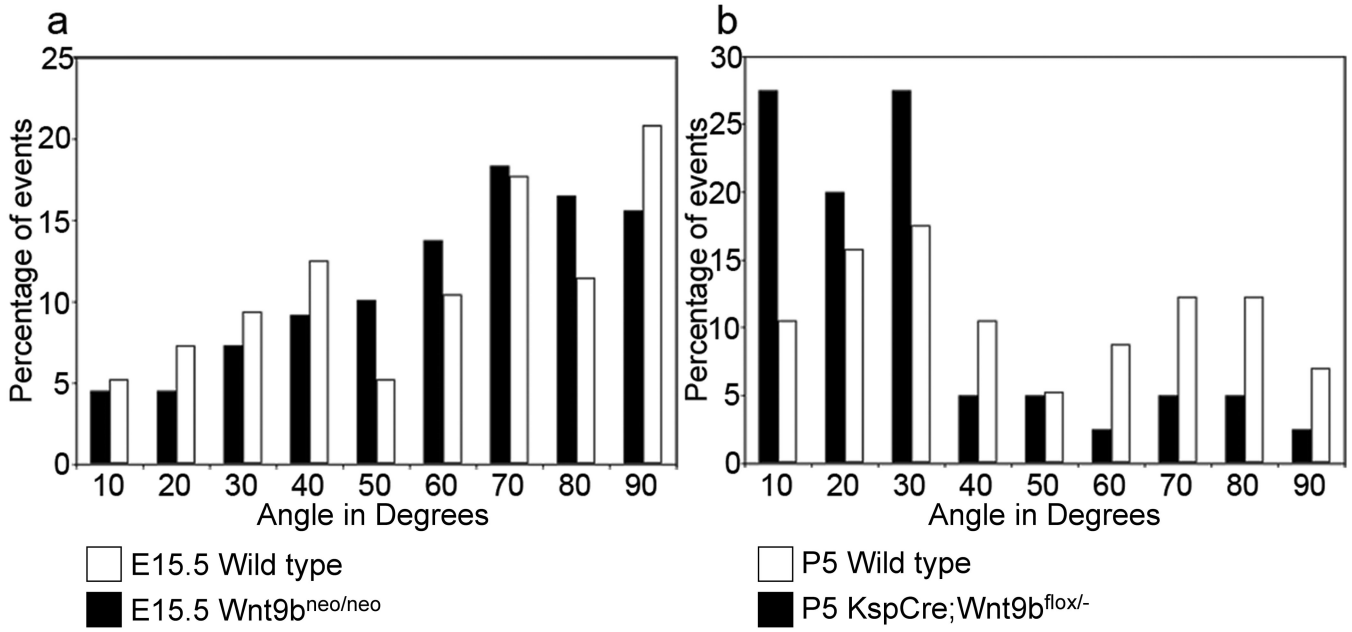

Figure 3. Cell division becomes oriented after birth in a Wnt9b–dependent process

(a) Graphical representation of the angle between the mitotic spindles and the longitudinal axis of DBA-positive tubules at E15.5 indicates that cell division in both wild type (black bars) and Wnt9b$^{neo/neo}$ tubules (white bars) is randomly oriented at E15.5 when compared to the expected random distribution by the Kolmogorov-Smirnov (KS) test. P > 0.55 for both wild type (N=109) and mutant (n=96). (b) At P5, the orientation of dividing cells in KspCre;Wnt9b$^{-/flox}$ DBA positive cells (white bars, n=50) is significantly different ($p < 0.01$, Mann-Whitney U test) from wild type (black bars, n=45) indicating that Wnt9b is necessary for orientation of cell division that occurs post-natally.

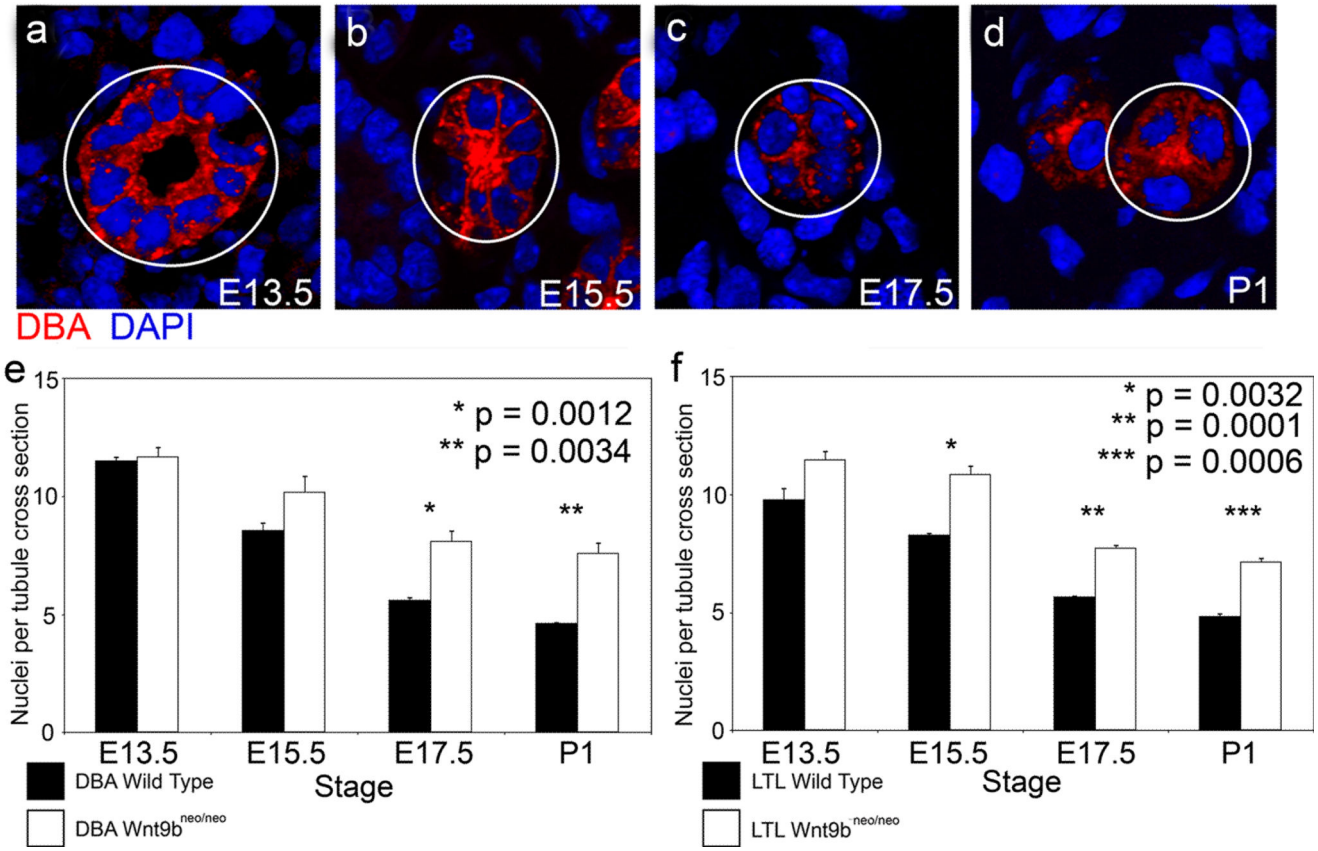

Figure 4. Wnt9b is required for the elongation and narrowing of kidney tubules

Representative sections through wild type DBA positive tubules from E13.5 (a), E15.5 (b), E17.5 (c), and P1 mice (d) showing the number of nuclei composing the wall of the tubule. Outlined tubules represent transverse sections. Quantitation reveals that the number of cells within the wall of wild-type collecting duct (black bars in e, n=563, 606, 844, and 692 for E13.5, 15.5, 17.5 and P1 respectively) and proximal tubules (black bars in f, n=425, 1030, 791, and 778 for E13.5, 15.5, 17.5 and P1 respectively) significantly decreases during the embryonic period. The number of cells within the tubule wall is significantly increased in Wnt9b mutant kidneys (white bars in e and f, n=384 or 412, 521 or 424, 915 or 902, and 665 or 635 for DBA or LTL at E13.5, 15.5 17.5 or P1 respectively). N=3 kidneys for each stage, tubular segment and genotype. Error bars represent standard error of the mean.

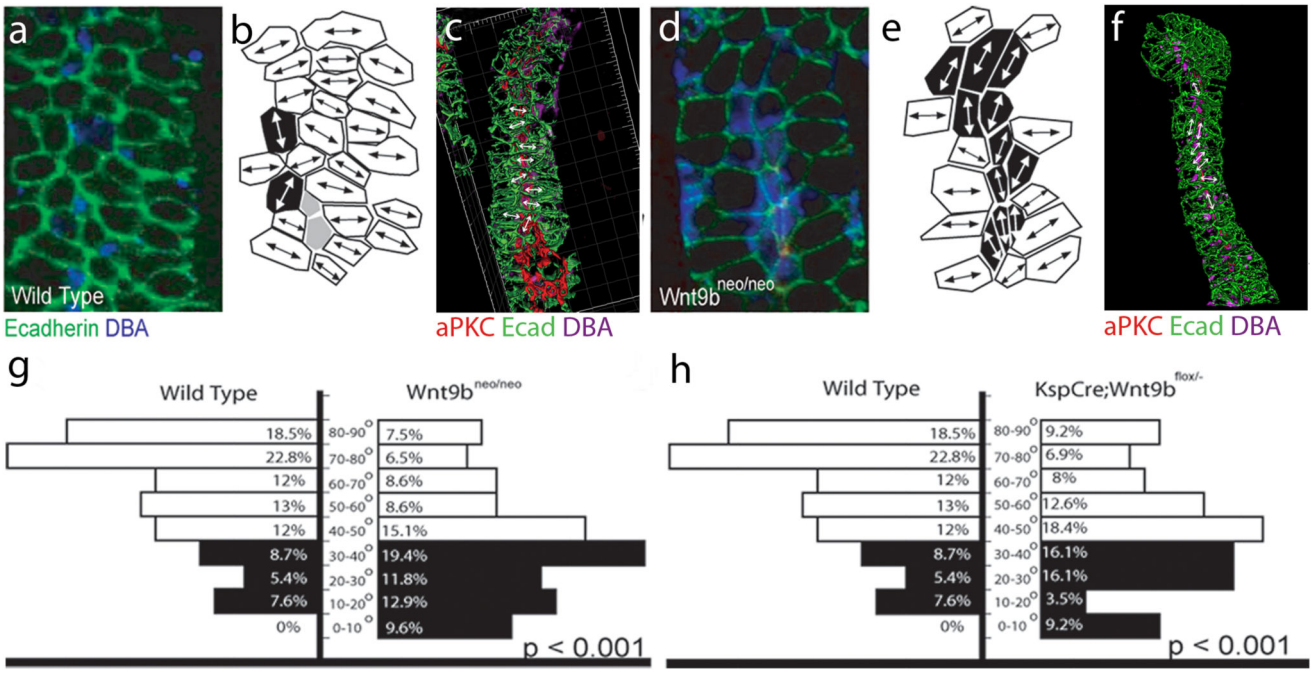

Figure 5.

Wnt9b is necessary for the orientation of polarized cells perpendicular to the axis of extension. Confocal images (a and d), cell outlines (b and e) and 3D reconstructions (c and f) of frontal sections through E15.5 wild type (a–c) and Wnt9b$^{neo/neo}$ (d–f) kidneys stained with anti-E-cadherin (green), anti-aPKC (red) and DBA (blue). In all cases, proximal is up and distal is down. The images in a and d represent sections just basal to the apical membrane as marked by anti-aPKC (red, not seen). Mediolaterally elongated cells are marked in white, proximal-distally elongated cells in black and unelongated cells in gray in b and e. The majority of wild-type cells are seen to be mediolaterally elongated perpendicular to the axis of extension (white in b). Wnt9b$^{neo/neo}$ cells are still elongated but the direction of elongation appears to be random (note increased number of black, proximal-distally elongated cells in e relative to b). (c and f) 3D reconstructions of Wild type (c) or Wnt9b$^{neo/neo}$ (f) e15.5 tubules to allow for visualization of cell orientation. Arrows indicate angle of orientation for marked cells. Quantitation of the angle of cellular elongation relative to the proximal distal axis of the tubule for wild-type (left in g and h) and Wnt9b$^{neo/neo}$ mutant (right in g) or KspCre;Wnt9b$^{-/flox}$ (right in h) cells. White bars indicate cells that are perpendicular to the axis of elongation (45–90°) while black bars represent cells that are parallel (0–45°). The percentage of cells within each 10 degree increment is indicated. There is a significant change in the orientation of the elongated cells between wild type and mutants. ($P<0.001$, KS test). The data was gathered from at least 3 different animals. The total number of oriented cells analyzed is 92, 86, or 93 for wild type, KspCre;Wnt9b$^{flox/-}$, or Wnt9b $^{neo/neo}$ respectively. Wild type cells are from littermate controls.

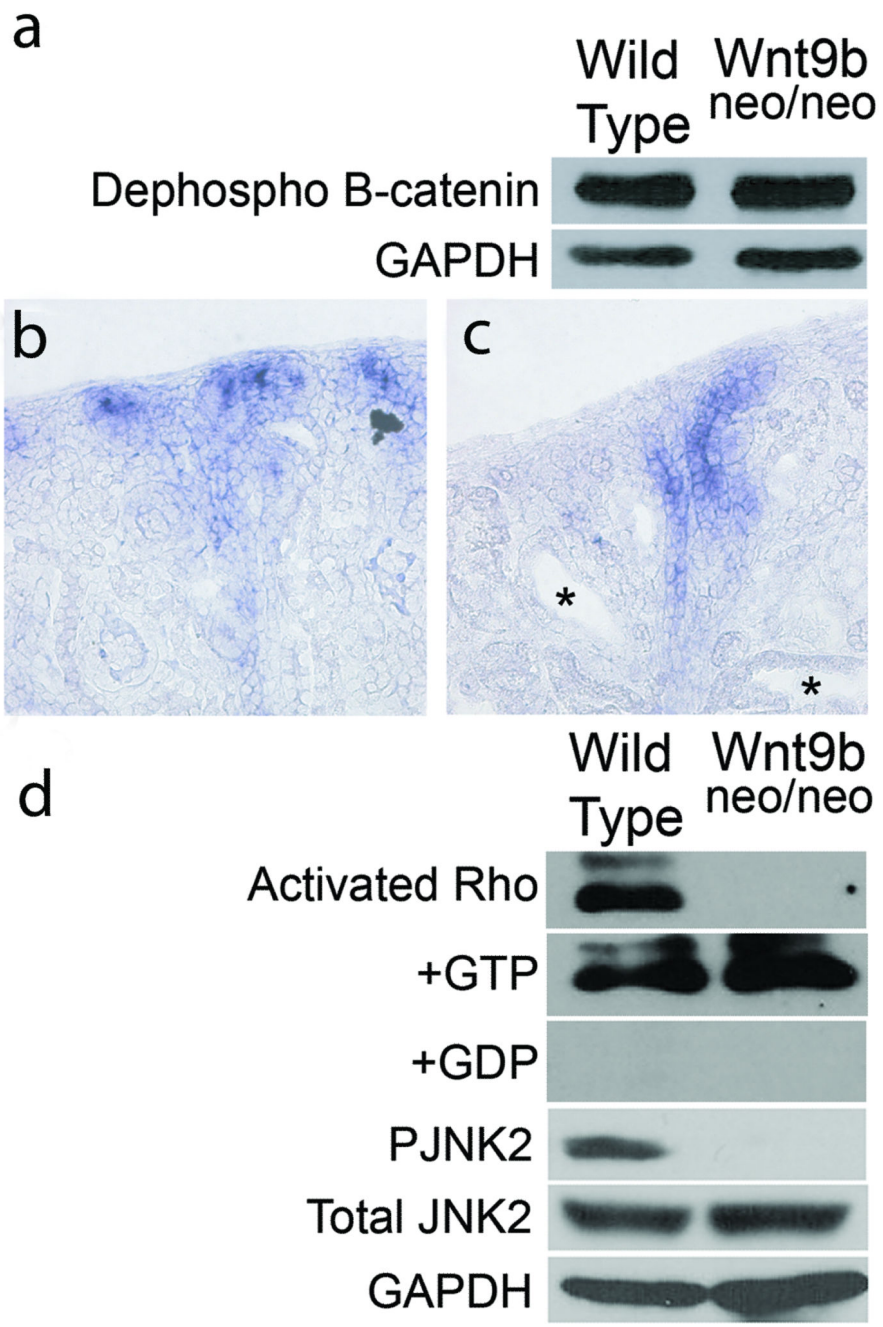

Figure 6. Wnt9b signals through the noncanonical pathway to regulate tubule diameter

Western blots of total protein extracted from wild-type and Wnt9b$^{neo/neo}$ kidneys probed with an antibody specific to the dephosphorylated (active) form of β-catenin show no significant differences in canonical Wnt activity compared to wild type (a). Section in situ hybridization with a probe for the β−catenin target axin-2 also shows no significant decrease in canonical activity in P1 Wnt9b$^{neo/neo}$ kidneys (c) compared to wild type (b). Note that there is no ectopic axin2 expression in cystic proximal tubules (asterisks in c). (d) Western blots indicate that activated Rho is significantly decreased in Wnt9b$^{neo/neo}$ kidneys at P1

relative to total (+GTP control) Rho levels. Addition of GDP (+GDP) to inactivate Rho was used as a negative control. Phosphorylated Jnk2 is also significantly decreased in the $Wnt9b^{neo/neo}$ kidneys at P1 relative to total levels of Jnk2 (d). Blots shown are representative examples of data gathered from at least 3 different blots from 3 independent protein extractions.